Fragility curves in reinforced concrete bridges considering the cumulative damage caused by seismic sequences

R. B. Flores [(1)], D. Tolentino [(2)]

[(1)] PhD Student, Departamento de Materiales Universidad Autónoma Metropolitana CDMX México, al2182800042@azc.uam.mx
[(2)] Professor, Departamento de Materiales Universidad Autónoma Metropolitana CDMX México, dantetl@azc.uam.mx

Abstract

An approach to estimate fragility curves considering the cumulate damage due to seismic sequences at the instant *t* of time is presented. The possible damage that the structure could accumulate is quantified by means of the maximum global drift. A stochastic process to simulate the possible seismic intensities and occurrences at the instant *t* is used for obtaining the structural demand under seismic sequences. It is considered that the occurrences between seismic events follow a stochastic Poisson process and the possible intensities are given by the seismic hazard at the site. The uncertainties related to the mechanic and geometric properties are taking into account by means of simulated properties. The proposed approach is illustrated in a continuous reinforced concrete bridge designed under the consideration that the bridge can develop a certain pre-established design drift equal to 0.003. The structure is located in transition soil (Type II) in Mexico City. Fragility curves are obtained for different time instants such as 0, 50, and 100 years after the bridge construction for different limits states. The fragility curves give relevant parameters in order to make decision of design, maintenance and repair, etc. The current Mexican design codes do not consider within design process the possible cumulative damage caused by seismic loadings and this topic is relevant in sites with high seismic occurrences such as Mexico City that recently occurred an earthquake in September 2017 leaving an economic loss of 9.2 billion dollars.

Keywords: fragility curves, cumulate damage, reinforced concrete bridge.

1. Introduction

The main aim of structural design is to satisfy a certain performance when demand occurs, in other words, when a structure is subjected to a seismic occurrence it is desired that the capacity would be greater than the demand. If a seismic occurrence appears and it produces that the system exceeds its yields behavior, the system loss capacity and certain damage are accumulated. In case that no repair actions in the structural system after the mentioned seismic loading, the structural damage could increase when the next seismic loading occurs. For the above, this study focuses to propose a rational way to take into account the cumulate damage caused by seismic loadings over time.

In Mexico, there are several bridges with more than 50 years of life service. Its structural design is developed to use the Mexican Transport Institute code (IMT, 2001) [1] and the manual of the American Association of state highway and transportation Officials (AASHTO, 2012) [2]. Unfortunately, it is necessary to improve the (IMT, 2001) [1] code with the aim to use a design code capable to consider the characterized of seismic loadings, mechanical properties of the materials, etc.

The most representative seismic occurrences that produced damage and caused collapses are San Fernando (1971), Mexico (1985), Loma Prieta (1989), Northridge (1994), Kobe (1995), Chile (2010) and Mexico (2017). Furthermore, one of the most important impacts that produce the collapse of a certain bridge are social, economic and politic losses. With the purpose of reducing these losses, it is necessary to propose rational assessments that consider into account the possible seismic loadings that could occur in a certain instant *t*. The aim of this kind of criterion is to extend the service life of the system.

Fragility curves have been studied for many of structural systems, in the particular way of bridges, fragility curves can be separated into Empirical [3,4] and analytical for MDOF considering continuous deck [5], continuous deck with simple support [6] and considering simple, fixed supports and elastomeric bearings [7]. For SDOF simply-supported with fixed bearings [8]. In the case of bridges under seismic loadings, many authors have been obtained fragility curves for the United States [9,10], Mexico [11,12], Asia [13] and Europe [14]. Moreover, fragility curves have been presented in order to take into account the effect of the cumulative damage caused by seismic loadings [15,16]. However, the works that consider the effect of cumulative damage under seismic sequences neglect the uncertainties related to mechanical and geometrical properties.

The objective of this work is to obtain the probability of exceeding a certain threshold considering the effect of the cumulative damage caused by sequences of seismic events. The approach takes into account the uncertainties related to seismic occurrences, geometric and mechanical properties. This work focuses on the drift threshold as a performance level indicator. The structure is located in Mexico City and designed to develop a threshold design equal to 0.003. The approach permits to identify the time instant to take a decision for maintenance.

2. Seismic motion

To estimate the cumulate damage, it is important to define the seismic loads that the structure could be exposed during its service life. According to the previous experiences (Mexico 1985 and 2017), the most adverse natural event in Mexico City is the seismic loading. In accordance to the above, there are two types of ground motions for structural analysis: a) recorded ground motions and b) synthetic ground motions. Given the lack of information about ground motion records, many authors have proposed approaches to simulate ground motions. By means of modulating process [17,18] defined as a product of determinist functions. It is known that this is a special case of [19]. After some years, [20] proposed a model to divide into segments the ground motion trying to represent the non-stationary process in the frequency content of the ground motion. However, [21] have made some improvement that considers the seismic motion as non-stationary Gaussian stochastic process, with statistical parameters depending on the magnitude and source-to-site distance and with the aim of associate seismic recorders of magnitude and source-to-site distance to simulated artificial seismic records [21]. According to the above, in this work, 1000 synthetic ground motions were simulated by using the approach of [21]. The synthetic ground motions correspond to transition soil in Mexico City. In Fig. 1 it is shown one simulated seismic record while in Fig. 2 it shows only 200 linear response spectra of the simulated seismic records.

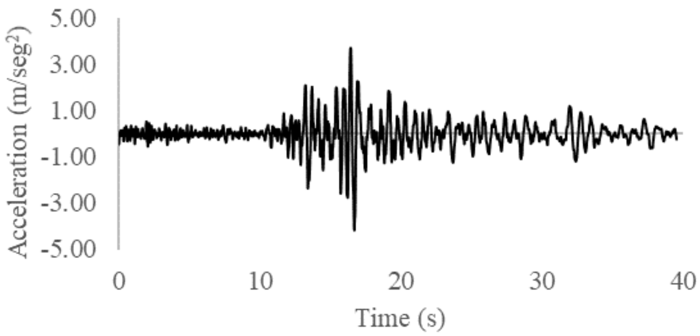

Fig. 1 – Synthetic ground motion record

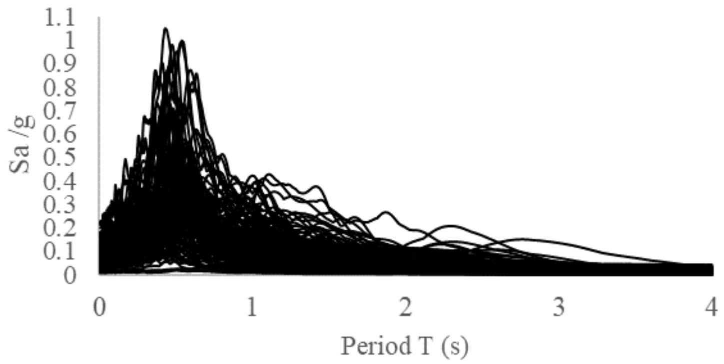

Fig. 2 – Response spectra for 200 synthetic ground motion records

3. Intensities and waiting times between seismic events

The seismic hazard curve, *SHC*, associated the fundamental period of the structure, *T*, with 5% of critical damping is represented by annual rate exceedance. In accordance with the *SHC* it is possible to simulate seismic intensities and it can be represented by Eq. (1).

$$\upsilon(y) = \upsilon_0 \left(\frac{y}{y_0}\right)^{-r} \left(\frac{y_{\max} - y}{y_{\max} - y_0}\right)^{\varepsilon} \tag{1}$$

where v_0 is the exceedance rate associated to y_0; y_0 is the minimum intensity to take into consideration, for this study (1 m/s^2); y_{max} is the maximum intensity of the seismic hazard curve; y is the range of exceedance rate of the seismic hazard curve; r and ε are functions setting parameters. Based on the above, the cumulative distribution function (CDF) is shown in Eq. (2). Fig. 3 shows the seismic hazard curve.

$$F_{(y)} = 1 - \frac{\upsilon(y)}{\upsilon_0} \tag{2}$$

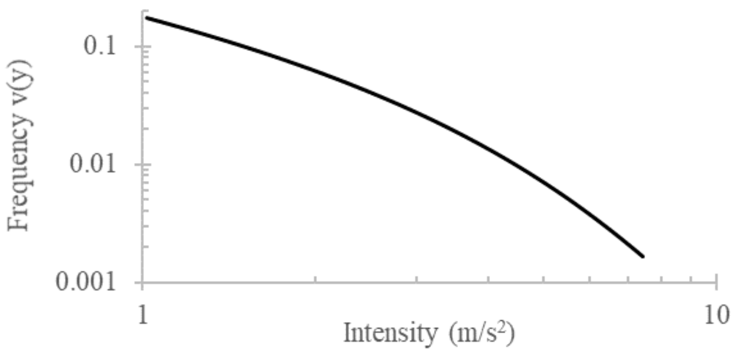

Fig. 3 – Seismic hazard curve

To determine the waiting time between seismic events it is supposed that these follow an exponential distribution [22] as Eq. (3).

$$F(u) = 1 - e^{-\upsilon_0 t} \tag{3}$$

After some mathematical arrangements, the waiting times are equal to Eq. (4).

$$T_i = -\left|\frac{\ln(u)}{\upsilon_0}\right| \tag{4}$$

where T_i is the waiting time between seismic events; u is a random variable with uniform distribution function. Such simulated intensity is associated with a simulated waiting time. An example of the above is shown in Fig. 4.

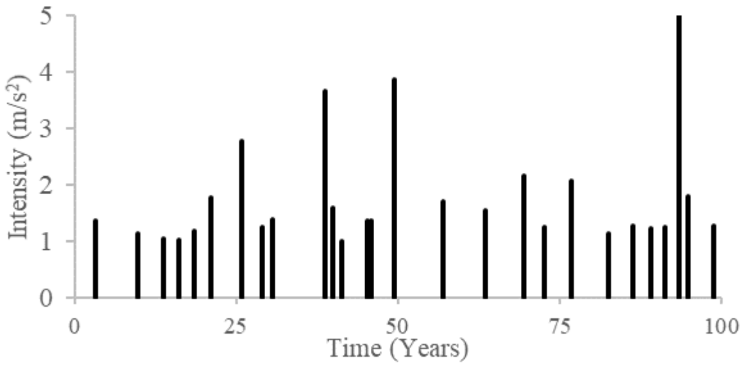

Fig. 4 – Simulated intensities and waiting times

4. Fragility curves

Fragility curves can be defined as the probability of exceeding a pre-established threshold for a given specific instant of time t. Considering that the structural demand follows a lognormal function distribution. The fragility curve at a certain time instant can be expressed as follows Eq. (5).

$$P(D_{|y,t} \geq d) = 1 - \Phi\left(\frac{\ln d - \ln \overline{D}_{|y,t}}{\sigma \ln D_{|y,t}}\right) \tag{5}$$

where d is the drift threshold and the mean value for a given an intensity at the instant of time t is computed by Eq. (6).

$$\overline{D}_{|y,t} = \exp(\sum_{i=1}^{n} \ln(D_{i|y,t}) / n) \tag{6}$$

which $D_{i|y,t}$ is the maximum drift for a given an intensity at the instant of time t; n is the number of samples and the standard deviation is computed by Eq. (7).

$$\sigma \ln D_{|y,t} = \sqrt{\sum_{i=1}^{n} (\ln D_{i|y,t} - \ln \overline{D}_{i|y,t})^2 / (n-1)} \tag{7}$$

5. Cumulative damage

The cumulate damage can be caused by several different environmental loads such as seismic loads, wind, waves, etc. In Mexico City, the main environmental load that produces damage in the structures are the earthquakes. The probabilistic approach to estimate the cumulate damage is shown in the next steps and illustrated how it is accumulating the seismic events over time, Fig. 5 is presented.

Step 1. Start with the interest instant of time t and the number of simulated model structures i-th.

Step 2. The i-th intensity and waiting time are related to i-th structural model by associating each intensity to a random synthetic ground motion affected by a factor $f = Sa_{sim}/Sa_T$, where Sa_{sim} is the simulated intensity and Sa_T is the spectral ordinary of the i-th ground motion at the structural fundamental period of the structure. Step 2 is repeated until the interest time t is reached.

Step 3. The structural response is calculated in terms of $D_{i|y,t}$ associated with the time instant t.

Step 4. The i-th synthetic ground motion is scale until the failure of the structure appears.

Step 5. The structural response is calculated in terms of $D_{i|y,t}$ associated with t.

For more analysis, steps 2 to 5 are repeated with the structure i-th= i-th+1 associated with the next time history of synthetic ground motion intensity i-th= i-th+1.

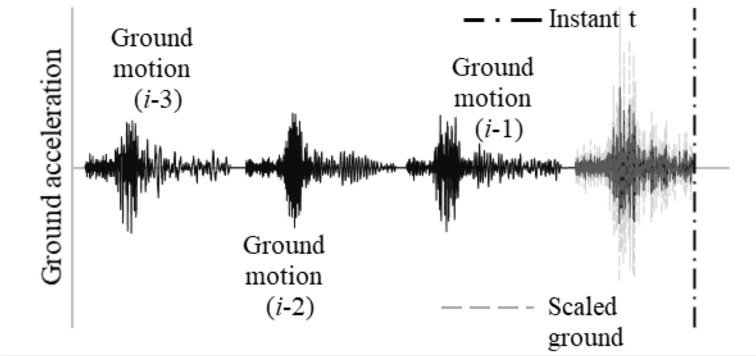

Fig. 5 – Successive seismic loading at the time instant t

It is important to mention that the damage is defined as the maximum drift. The steps illustrate the process of cumulative damage starting with defined t that represents the instant of interest t. It is supposed that the simulated structures have been done taking into account different uncertainties such as geometric and mechanical properties [23,24]. As well as it is important to express that for a time equal to 0 the structure is taken as new without damage. The i-th intensity is related to a random synthetic ground motion affected by a factor that results in the relationship between simulated intensity and spectral acceleration associated to structural fundamental period T. After scaling the history of synthetic seismic events associated with intensity and time occurrence until the instant of interest t. The last seismic event (see Fig. 5) is scaled until the failure of the structure appears, the criterion used for failure is the dynamic instability [25-27].

6. Application example

The approach to estimate fragility curves considering the cumulate damage at the time instant t is illustrated for a continuous reinforced concrete bridge located in transition soil Mexico City and designed with Mexican City code (NTC, 2017) [28] and AASHTO code (AASHTO, 2012) [2]. The bridge is 130 m length and 18.2 m width. It has two middle spans of 35 m and two lateral spans of 30 m (see Fig. 6). Moreover, five circular columns of 7.0 m height, 18.2 m of transversal length with four lines-roadway of 3.6 m width (see Fig. 7). A compressive concrete strength f′c=39.2 MPa in beams type AASHTO, f′c=24.5 MPa in slab and f′c=29.4 MPa in columns and cap beams were used. In addition, it is considered that the continuous bridge can perform a pre-established drift threshold equal to 0.003. The geometric sections with its correspond reinforcement steel for flexural moment and shear are shown in Fig. 8. The structure has a fundamental period T equal to 0.48 s.

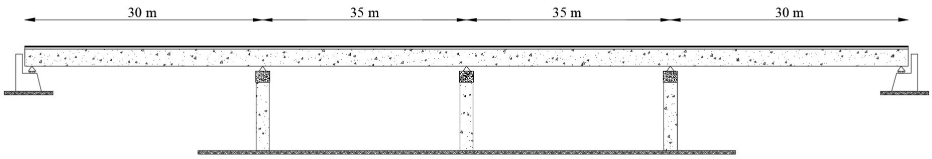

Fig. 6 – Longitudinal section

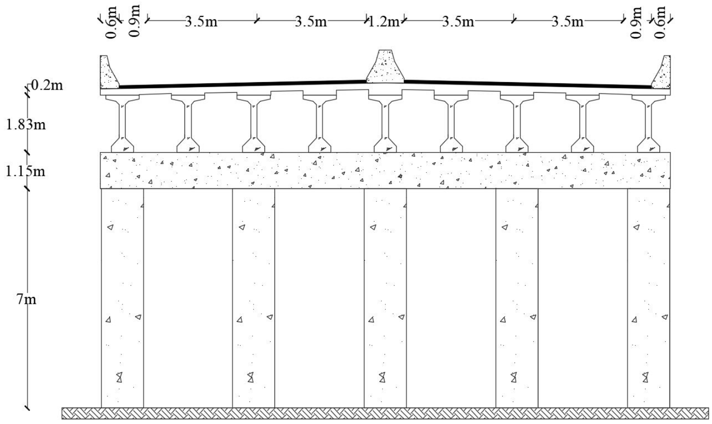

Fig. 7 – Transversal section

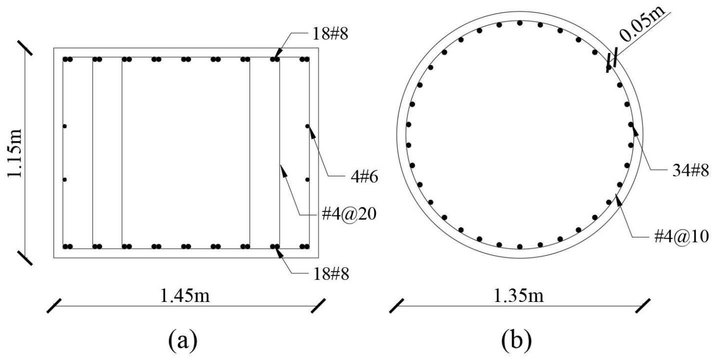

Fig. 8 – Geometric section and steel reinforcement (a) beam caps (b) columns

The inelastic response was computed with Ruaumoko 3D software, taking into account concentrated plasticity at the end of both extremes of the frame. In contrast, the deck only transmits dead load. The structural failure is considering by the appearance of plastic hinge in all columns. The Modified Takeda hysteresis rule is used. Ruaumoko 3D software solves the dynamic equilibrium equation using Newmark constant acceleration method. As previously mentioned, in this study it is considering the uncertainties related to the geometrical and mechanical properties. Table 1 shows the uncertainties related to the geometrical properties and Table 2 shows the uncertainties related to mechanical properties. Ruaumoko 3D software characterizes the plastic hinge with moment-curvature. Hence, mechanical characterization was used for stress-strain curve steel [29] and [30] for stress-strain curve reinforced concrete.

Table 1 Geometrical uncertainties

Item	Mean μ (m)	Standard deviation σ (m)	Ref.
Beams caps base	1.4525	0.0038	[23]
Beams caps height	1.1705	0.0129	[23]
Column width	1.3515	0.0064	[23]
Slab thickness	0.2076	0.0066	[23]
Effective depth	+0.0102	0.0127	[24]

Table 2 Mechanical uncertainties characterization

Variable	Item	Mean μ	Standard deviation σ	Ref.
f´c (MPa)	Column width	35.89	5.14	[23]
	AASHTO beams	47.87	4.35	[23]
	Slab	30.32	3.63	[23]
fy (MPa)	Ø≤1/2"	452.10	36.87	[29]
	Ø>1/2"	440.17	16.58	[29]
fu (MPa)	Ø≤1/2"	729.17	29.12	[29]
	Ø>1/2"	713.87	16.28	[29]

f'c = simple compression stress of concrete
fy = yield stress of steel, fu= ultimate stress of steel

6.1 Structural demand

The structural demand is obtained based on nonlinear dynamic analysis "step by step" at different time instants. The cumulative damage under seismic sequences is obtained using the procedure in section 5, as mention before, the structural demand is represented as the maximum drift presented at the deck of the bridge, Fig. 9 shows the median of the structural demand for time instants equal to 0, 50 and 100 years after the bridge construction, $\overline{D}_{i|y,t}$, it can be noted in Fig. 9 that the mean of the demand for a given intensity at the instant of interest time, t, increases owing to the increment of seismic sequences, it means that the structure is subject to greater seismic events over time. Furthermore, it can be noticed that the intensity of 0.1 sa/g for the instant time 0 produces damage and an initial cumulate damage for the time instants of 50 and 100 years. Moreover, it is obtained a value of $\overline{D}_{i|y,t}$ equal to 0.00153 in 0.1 sa/g for 100 years while for a structure without damage $\overline{D}_{i|y,t}$ is equal to 0.000305. The above represents an increase of 401.6%. In addition, most of the simulated structures presented their failure after reach the 0.9 sa/g.

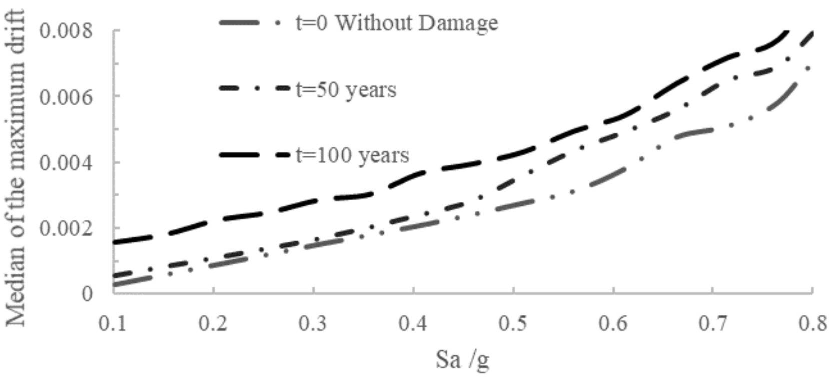

Fig. 9 – Median of the natural logarithm of demand for 0, 50 and 100 years

6.2 Fragility curves over time

Fragility curves are obtained for different time instants such as 0, 50 and 100 years after the bridge construction. Fig. 10,11 and 12 show the fragility curves for the drift thresholds 0.001, 0.003 and 0.006 respectively. Fig. 10 is focus in the probability exceedance of drift threshold 0.001 for 0 50 and 100 years life expectancy in bridges shows that a seismic intensity of 0.250 sa/g is needed to reach a probability exceedance of 0.80 in 50 years while the same probability for the case of 100 years is presented for the intensity equal to 0.1 sa/g. The above represents 150% of increment. Fig. 11 is focused on the design drift threshold 0.003, it illustrates that the probability exceedance 0.35 Sa/g are 0.02743, 0.08612 and 0.45240 for the time instant of 0, 50 and 100 years. According to the above, the probability increases 213.96% between 0 and 50 years and for the time instants of 50 to 100 years, the probability of exceedance increases 325.31%. Fig. 12 shows fragility curves with a probability of exceeding a threshold equal to 0.006 and shows that the intensity equal to 0.8 sa/g the structure presents a probability equal to 0.6050, 0.7178 and 0.8153 for 0, 50 and 100 years of the bridge construction, respectively. The above represents high probability of being increase the selected threshold.

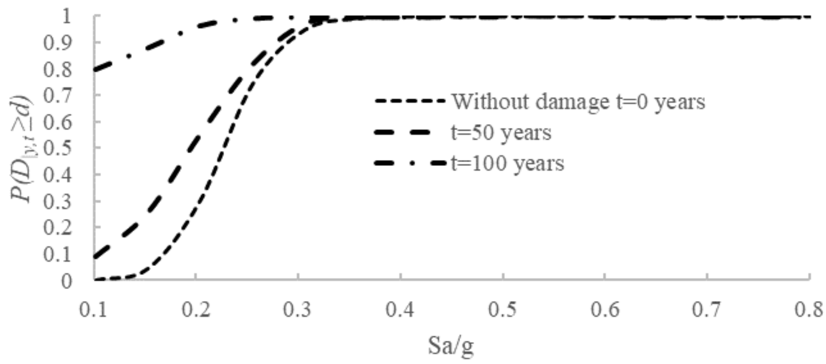

Fig. 10 – Fragility curves of 0,50 and 100 years for drift threshold 0.001

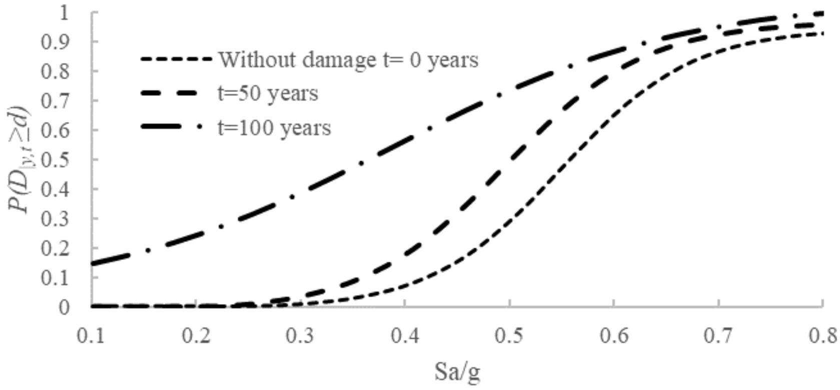

Fig. 11 – Fragility curves of 0,50 and 100 years for drift threshold 0.003

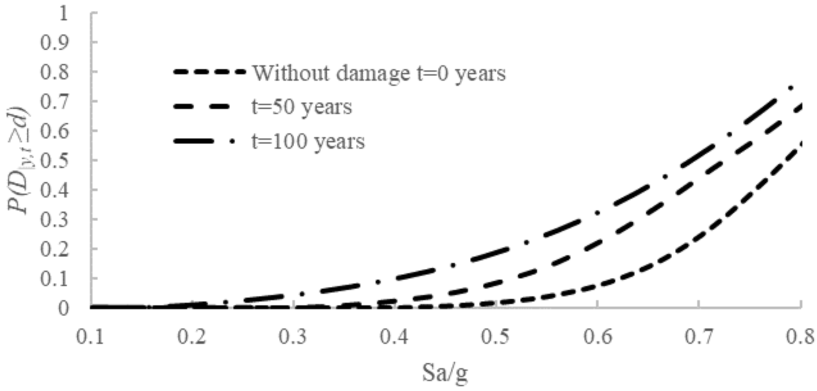

Fig. 12 – Fragility curves of 0,50 and 100 years for drift threshold 0.006

7. Conclusions

An approach was to obtain fragility curves taking into account important uncertainties related to seismic occurrences, mechanical and geometric at different time instant is presented. The approach can be used for different environmental loads such as wind, waves and others phenomena such as corrosion, scour, erosion, etc. The effect of the cumulative damage caused by the occurrence of seismic sequences is noted with the increment of the probability of exceeding for the same intensity at different time instants.

The approach was illustrated in a continuous reinforced bridge designed to perform a drift threshold equal to 0.003. The cumulate damage was quantified for different time instants (0, 50 and 100 years) taking into account the uncertainties related to mechanical and geometrical properties. Fragility curves were obtained for different drift thresholds such as 0.001 0.003 and 0.006. Based on the results, the 0.003 threshold design is recommended because it requires high intensity such as 0.35 sa/g to exceed the threshold design at the instants of 0 and 50 years. However, it is necessary to make an inspection in order to detect potential elements to be repaired at the instant of time equal to 100 years.

8. Acknowledgements

The National Science and Technology Council of Mexico (CONACyT) granted a Ph.D. fellowship for the first author is gratefully acknowledged. The second author acknowledges the support of Programa para el Desarrollo Docente, para el Tipo Superior (PRODEP) through the project UAM-PTC-685. Moreover, both authors thank Universidad Autónoma Metropolitana.

9. Copyrights

10. References

[1] Instituto Mexicano del Transporte (2001). *Proyecto de puentes y estructuras*, (in Spanish).

[2] American Association of State Highway and Transportation Officials (2012). *Standard specifications for highway bridges*. American Association of State Highway and Transportation Officials.

[3] Basöz NI, Kiremidjian AS, King SA, Law KH (1999): Statistical analysis of bridge damage data from the 1994 Northridge, *Earthquake Spectra,* **15**(1), 25–54.

[4] Elnashai AS, Borzi B, Vlachos S (2004): Deformation-based vulnerability functions for RC bridges. *Structural Engineering and Mechanics,* **17**(2), 215–244.

[5] Lupoi A, Franchin P, Pinto PE, Monti G (2005): Seismic design of bridges accounting for spatial variability of ground motion. *Earthquake Engineering Structural Dynamics,* **34**(4–5), 327–348.

[6] Padgett JE, DesRoches R (2009): Retrofitted bridge fragility analysis for typical classes of multispan bridges. *Earthquake Spectra,* **25**(1), 117–141.

[7] Zhang J, Huo Y, Brandenberg SJ, Kashighandi P (2008): Effects of structural characterizations on fragility functions of bridges subject to seismic shaking and lateral spreading. *Earthquake Engineering and Engineering Vibration,* **7**(4), 369–382.

[8] Shirazian S, Ghayamghamian MR, Nouri GR (2011) Developing of fragility curve for two-span simply supported concrete bridge in near-fault area. *World Acad Sci Eng Technol* 51:571–575.

[9] Choi E, Desroches R, Nielson, B (2004): Seismic fragility of typical bridges in moderate seismic zones. *Engineering Structures*, **26**(2), 187–199.

[10] Mackie KR, Stojadinovic B (2007): R-Factor Parameterized Bridge Damage Fragility Curves. *Journal of Bridge Engineering ASCE*, **12**(4).

[11] Ruiz-García J, Negrete M (2008): Drift-based fragility assessment of confined masonry walls in seismic zones. *Engineering Structures,* 31 (2009) 170-181.

[12] Olmos BA, Jara JM, Gómez MCTJ, Jara M (2016): Influence of RC jacketing on the seismic vulnerability of RC bridges. *Engineering Structures,* 123 (2016) 236–246.

[13] Lee SM, Kim TJ, Kang SL (2007): Development of fragility curves for bridges in Korea. *KSCE Journal of Civil Engineering, Korean Society of Civil Engineers*, **11**(3), 165-174.

[14] Moschonas IF, Kappos AJ, Panetsos P, Papadopoulos V, Makarios T, Thanopoulos P (2009): Seismic fragility curves for Greek bridges: methodology and case studies. *Bulletin of Earthquake Engineering, Springer Netherlands*, **7**(2), 439-468.

[15] Panchireddi B, Ghosh J (2019): Cumulative vulnerability assessment of highway bridges considering corrosion deterioration and repeated earthquake events. *Bulletin of Earthquake Engineering, Springer Netherlands*, **17**(3), 1603-1638.

[16] Tolentino D, Marquez-Dominguez S, Gaxiola-Camacho R (2019): Fragility Assessment of Bridges Considering Cumulative Damage Caused by Seismic Loading. *KSCE Journal of Civil Engineering*.

[17] Bolotin V (1960): Statistical Theory of Aseismic Design of Structures. *Proceedings of the Second World Conference on Earthquake Engineering*, 1365-1374.

[18] Aming, Ang Amin M, and Ang, A H-S (1968): A Nonstationary Stochastic Model for Strong Motion Earthquakes, *Journal of the Engineering Mechanics Division*, ASCE. **94**(2), 559-583.

[19] Priestley MB (1965): Evolutionary Spectra and Non-stationary Processes. R. Statist. Soc. B, 1965, pp 204-237.

[20] Grigoriu M, Ruiz SE, Rosenblueth E (1988): The Mexico Earthquake of September 19, 1985, Nonstationary Models of Seismic Ground Acceleration. *Earthquake Spectra*, **4**(3), 551-568.

[21] Alamilla J, Esteva L, Garcia-Perez J, Diaz-Lopez O (2001a): Evolutionary properties of stochastic models of earthquake accelerograms. Their dependence on magnitude and distance, *Journal of Seismology,* **5**, 1-21.

[22] Benjamin JR, Cornell CA (1970): *Probability, Statistics and Decision for Civil Engineers*. McGraw-Hill, pp. 243.

[23] Nowak A, Rakoczy A, Szeliga E (2013): Revised Statistical Resistance Models for R/C Structural Components, *ACI Symposium Publication*, **284**, 1-16.

[24] Ellingwood B, Galambos TV, McGregor JG, Cornell CA (1980): Development of a Probability Based Load Criterion for American National Standard A58, *NBS Special Report 577*, U.S. Department of Commerce, National Bureau of Standards.

[25] Jalayer F, Cornell CA (2009): Alternative non-linear demand estimation methods for probability based seismic assessments. *Earthquake Engineering and Structural Dynamics*, John Wiley & Sons Inc, Vol. 38. pp. 951–972.

[26] Tolentino D, Ruiz SE. (2015): Time-dependent confidence factor for structures with cumulative damage, *Earthquake Engineering Research Institute*, **31**(1), 441.

[27] Tolentino D, Carrillo-Bueno CA (2018): Evaluation of structural reliability for reinforced concrete buildings considering the effect of corrosion, *KSCE Journal of Civil Engineering*, Korean Society of Civil Engineers, **22**(4), 1344-1353.

[28] Normas Técnicas Complementarias del Reglamento de Construcción de la Ciudad de México (2017). *Gaceta Oficial del Departamento de la Ciudad de México*, (In spanish).

[29] Rodríguez M, Botero JC (1996): Aspectos del comportamiento sísmico de estructuras de concreto reforzado considerando las propiedades mecánicas de aceros producidos en México. *Serie azul del instituto de ingeniería*, UNAM. No. 575.

[30] Mander JB, Priestley MJN, Park R (1988): Theoretical Stress-Strain Model for Confined Concrete. *Journal of Structural Engineering*, **114**(8), 1804-1826.

